Journal of Oleo Science

doi : 10.5650/jos.ess17032
J. Oleo Sci. **66**, *(9) 939-950 (2017)*

Development and Optimization of Orally and Topically Applied Liquid Crystal Drug Formulations

Wesam R. Kadhum[1], Tomoki Hada[1], Ichiro Hijikuro[2], Hiroaki Todo[1] and Kenji Sugibayashi[1,*]

[1] *Faculty of Pharmacy and Pharmaceutical Sciences, Josai University, 1-1 Keyakidai, Sakado, Saitama 350-0295, JAPAN*
[2] *Farnex Incorporated, Tokyo Institute of Technology Yokohama Venture Plaza, 4259-3, Nagatsuta, Midori-ku, Yokohama 226-8510, JAPAN*

Abstract: Liquid crystal (LC)-forming lipids represent an important class of biocompatible amphiphiles and their application extends to cosmeceutical, dietary, and pharmaceutical technologies. In the present study, we aimed to develop strategies for designing and optimizing oral and topical LC formulations by evaluating their *in vitro* and *in vivo* drug absorption performances. C_{17}-Monoglycerol ester (MGE) was used as a LC-forming lipid. *p*-Amino benzoic acid, methyl PABA, ethyl PABA, and sodium fluorescein were selected as drug models with different physiochemical properties. Various oral and topical LC formulations were designed based on changes in the LC forming lipid contents in the formulations and entrapped with different physiochemical properties of the drugs. The LC phase structures were evaluated using small-angle X-ray scattering (SAXS). The drug-release profiles from LC formulations were determined using a dialysis membrane method. *In vivo* oral absorption of LC formulations was conducted in Wistar rats. Furthermore, the skin penetration of drugs from LC formulations was investigated by *in vitro* skin permeation studies. As a result, although the release profile was influenced by changes in MGE concentration, it was more dramatically influenced by changes in the physiochemical properties of the entrapped drugs. Drug absorption after oral and topical administration of LC formulations was dramatically affected by the concentration of MGE. The concentration of LC-forming lipid and the physiochemical properties of entrapped drugs are key issues for good performance of the LC formulations in various pharmaceutical applications. The present results could enable researchers to manipulate LC formulation approaches intended to improve the oral absorption and skin permeation of drugs.

Key words: liquid crystal, C_{17}-monoglycerol ester, lipid concentration, oral absorption, skin penetration

1 Introduction

Recently, increasing attention has been paid to liquid crystal (LC) formulations, such as cubosomes and hexosomes, because of their remarkable structural complexity and usefulness in various pharmaceutical applications. LC-forming lipids represent an important class of biocompatible amphiphiles, and their application extends to several fields, such as cosmeceutical, dietary, and pharmaceutical technologies[1-3]. LC phases are able to accommodate biologically active molecules such as vitamins, enzymes, and other proteins[4,5]. The advantages of LC formulations as a drug-delivery system are their high biocompatibility and the self-assembly ability of their structure. This ability opens new possibilities for pharmaceutical applications[6]. Several studies have reported the usefulness of LC formulations to enhance the drug absorption after oral and transdermal application[7-10]. Ali *et al.* reported enhancing effect of orally administered poorly water soluble drugs of spironolactone (estimated log $K_{octanol/water}$: 2.9 and molecular weight (MW): 417) and nifedipine (estimated log $K_{octanol/water}$: 2.2 and MW: 346) with reverse bicontinuous cubic phase of monoolein[11]. Nguyen *et al.* investigated the ability of nanostructured reverse bicontinuous cubic phase of monoolein to sustain the absorption of a poorly water soluble drug, cinnarizine (estimated log $K_{octanol/water}$: 5.8 and MW: 369) after oral administration[10]. In addition, Cohen-Avrahami *et al.* examined skin permeation-enhancement effect of a hydrophilic drug, sodium diclofenac (log $K_{octanol/water}$: -0.1 and MW: 318) with reversed hexagonal lyotropic liquid crystals containing a skin permeation enhancer[12]. Lopes *et al.* investigated transdermal delivery of cyclosporin A (log $K_{octanol/water}$: 2.92 and MW: 1202) with reverse cubic and hex-

*Correspondence to: Kenji Sugibayashi, Faculty of Pharmacy and Pharmaceutical Sciences, Josai University, 1-1 Keyakidai, Sakado, Saitama 350-0295, JAPAN
E-mail: sugib@josai.ac.jp
Accepted March 31, 2017 (received for review February 7, 2017)
Journal of Oleo Science ISSN 1345-8957 print / ISSN 1347-3352 online
http://www.jstage.jst.go.jp/browse/jos/ http://mc.manusriptcentral.com/jjocs

agonal phase of monoolein and also reported another successful application with the combination of vitamin K (estimated log $K_{octanol/water}$: 11.7 and MW: 451) and hexagonal phase of monoolein[8]. Furthermore, in our previous studies[13, 14], we demonstrated successful improvement in drug absorption after oral and transdermal application with LC formulations that composed with glyceryl 5,9,13-trimethyltetradec-4-enoate (MGE; Fig. 1), and the enhancement effect of these formulations was dramatically affected by the type of LC-forming lipids. MGE was easy-to-handle due to its low viscosity at 25℃ compared to glyceryl monooleate (GMO) and phytantriol (PHT) and it showed better drug absorption enhancement effects. However, no studies have investigated the effect of several factors such as physiochemical properties of the entrapped drugs and concentration of LC-forming lipids and LC phase structure on the enhancement effect of orally and topically administered drugs. Therefore, in the present study, MGE was selected as an LC-forming lipid. *p*-Amino benzoic acid (PABA) and its prodrugs, methyl *p*-aminobenzoate (M-PABA) and ethyl *p*-aminobenzoate (E-PABA) (Table 1) were selected as drug models with different lipophilicities to understand the effect of the lipophilicity changes on the drug absorption performance of LC formulations. On the other hand, for transdermal LC formulations, only hydrophilic sodium fluorescein (Na-FL) was selected as a model drug and was entrapped with different concentrations of MGE. Overcoming the stratum corneum barrier to cutaneously deliver hydrophilic drugs is one of the major challenges in the field of dermatologic therapy; therefore, Na-FL was used as a well-known hydrophilic and mal-absorbed model drug in this study. Thus, in the present study we aimed to develop strategies for designing and optimizing oral and topical LC formulations by evaluating the effect of these factors on the drug absorption from LC formulations.

2 Materials and methods

2.1 Materials

MGE (purity: >99.56%) was obtained from Farnex Co., Inc. (Yokohama, Japan). PABA, M-PABA, and E-PABA were purchased from Kanto Chemical Co., Inc. (Tokyo, Japan). Na-FL was purchased from Tokyo Chemical Industry Co., Ltd. (Tokyo, Japan). A surfactant, Pluronic® F127, was purchased from Sigma-Aldrich (St. Louis, MO, USA). Other reagents and solvents were of special grade or HPLC grade and used without further purification.

2.2 Preparation of oral and topical LC formulations

Table 2 lists the oral and topical LC formulations used in this study. These formulations were designed based on changing the concentration of MGE in the formulations and entrapped with drugs with different physiochemical properties. The mixture was dispersed using a homogenizer (Polytron PT-MR 3000; Kinematica Inc., Littau, Switzerland). The dry powder LC formulations were prepared using a freeze dryer (Labcono FZ-18; Asahi Life Science Co. Ltd., Tokorozawa, Saitama, Japan).

2.3 Measurement of particle size and zeta potential

The particle size and zeta potential of LC formulations were determined using a dynamic light scattering Nano-ZS ZEN3600 Zetasizer (Malvern Instruments Ltd., Worcestershire, U.K.). LC samples were diluted in distilled water and shaken using a vortex mixer prior to measurement.

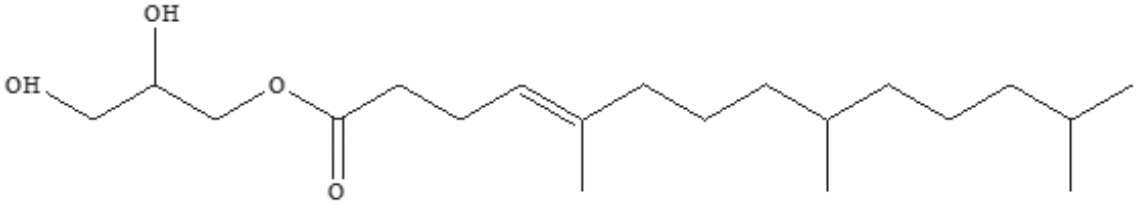

MGE

Fig. 1 Chemical structures of C_{17}-monoglycerol ester (MGE).

Table 1 Physicochemical properties of the compounds used in the present study.

	Abbreviation	M.W.	ClogP
p-Amino benzoic acid	PABA	137.14	0.98
Methyl *p*-aminobenzoate	M-PABA	151.17	1.39
Ethyl *p*-aminobenzoate	E-PABA	165.19	1.93
Sodium fluorescein	Na-FL	376.27	−2.02

Table 2 Composition of oral and topical LC formulations.

Formulation code	Composition of oral LC formulations
OP5*	PABA solution containing 5% Pluronic® F127 and 5% MGE
OP10	PABA solution containing 5% Pluronic® F127 and 10% MGE
OP20	PABA solution containing 5% Pluronic® F127 and 20% MGE
OP30*	PABA solution containing 5% Pluronic® F127 and 30% MGE
OP10D	PABA dry powder formulation containing 5% Pluronic® F127, 10% MGE, 10% mannitol and 1% ethanol
OP20D*	PABA dry powder formulation containing 5% Pluronic® F127, 20% MGE, 10% mannitol and 1% ethanol
OM5*	M-PABA solution containing 5% Pluronic® F127 and 5% MGE
OM10	M-PABA solution containing 5% Pluronic® F127 and 10% MGE
OM20	M-PABA solution containing 5% Pluronic® F127 and 20% MGE
OM30*	M-PABA solution containing 5% Pluronic® F127 and 30% MGE
OM10D	M-PABA dry powder formulation containing 5% Pluronic® F127, 10% MGE, 10% mannitol and 1% ethanol
OM20D*	PABA dry powder formulation containing 5% Pluronic® F127, 20% MGE, 10% mannitol and 1% ethanol
OE5*	E-PABA solution containing 5% Pluronic® F127 and 5% MGE
OE10	E-PABA solution containing 5% Pluronic® F127 and 10% MGE
OE20	E-PABA solution containing 5% Pluronic® F127 and 20% MGE
OE30*	E-PABA solution containing 5% Pluronic® F127 and 30% MGE
OE10D	E-PABA dry powder formulation containing 1% Pluronic® F127, 10% MGE, 10% mannitol and 1% ethanol
OE20D*	M-PABA dry powder formulation containing 5% Pluronic® F127, 20% MGE, 10% mannitol and 1% ethanol
TF5**	Na-FL solution containing 5% Pluronic® F127 and 5% MGE
TF10	Na-FL solution containing 5% Pluronic® F127 and 10% MGE
TF20	Na-FL solution containing 5% Pluronic® F127 and 20% MGE
TF30	Na-FL solution containing 5% Pluronic® F127 and 30% MGE
TF40	Na-FL solution containing 5% Pluronic® F127 and 40% MGE
TF50**	Na-FL solution containing 5% Pluronic® F127 and 50% MGE

The concentration of PABA, M-PABA, or E-PABA solution was 10 mM and the concentration of Na-FL solution was 5 mM
Formulation code: O = Oral formulation; T = Topical formulation; P = PABA; M = M-PABA; E = E-PABA; F = Na-FL; D = Dry powder; Number = Percentage of MGE.
*: Rejected oral formulations.
**: Rejected topical formulations.

2.4 SAXS measurement

SAXS measurement of dispersed formulations was performed using a Nano-Viewer (Rigaku, Tokyo, Japan) with a Pilatus 100K/RL 2D detector. The X-ray source was Cu Kα radiation with a wavelength of 1.54 Å and operating at 45 kV and 110 mA. The sample-to-detector distance was set at 375 mm. Each sample was placed into a vacuum-resistant glass capillary cell and exposed at 25℃ for 10 min. The SAXS pattern obtained was plotted against the scattering vector length, $q = (4\pi/\lambda)\sin(\theta/2)$ where θ is the scattering angle.

2.5 Release experiment

A dialysis membrane (molecular weight cut-off; 2,000–14,000 Da, Sanko Junyaku Co., Tokyo, Japan) was set in a vertical-type diffusion cell (effective diffusion area: 0.95 cm^2) and the receiver chamber was maintained at 32℃. Phosphate-buffered saline (PBS; pH 7.4) was applied to the receiver chamber. Drug (PABA, M-PABA, E-PABA or Na-FL) solution (1.0 mL) or its LC formulation (1.0 mL) was applied to the donor cell to start the release experiment. An aliquot (500 μL) was withdrawn from the receiver chamber, and the same volume of PBS was added to the chamber to keep the volume constant. The amount of PABA, M-PABA, and E-PABA released was determined using an HPLC (Shimadzu Ltd., Kyoto, Japan). In case of Na-FL, the released amount was determined using a fluorescence spectrophotometer (Shimadzu Ltd., Kyoto, Japan). The cumulative % of drug released was plotted against the square root of time (Higuchi's plot)[15].

2.6 Animals

Male hairless (WBM/ILA-Ht) and male Wistar (Slc) rats were purchased either from Life Science Research Center,

Josai University (Sakado, Saitama, Japan) or Ishikawa Experiment Animal Laboratories (Fukaya, Saitama, Japan). Animals were housed in temperature-controlled rooms (25 ±2℃) with a 12 h light-dark cycle (07:00–19:00 h). The rats were allowed free access to food (Oriental Yeast Co., Tokyo, Japan) and tap water. The animal experiment protocol was approved by the Animal Care and Use Committee of Josai University (Sakado, Saitama, Japan).

2.7 HPLC conditions

The *in vivo* or *in vitro* study sample (50 μL) was mixed with the same volume of acetonitrile (to precipitate plasma proteins) containing methyl paraben (10 μg/mL) as an internal standard and centrifuged (5 min, 4℃). The obtained supernatant (20 μL) was injected into an HPLC system (Shimadzu, Kyoto, Japan), which consisted of a system controller (CBM-20A), pump (LC-20AD), auto-sampler (SIL-20AC), column oven (CTO-20A), UV detector (SPD-M20A), and analysis software (LC Solution). The column was an GL Sciences Inc. ODS-3 (5 μm, 4.6×250 mm) (Nihon Waters K.K., Tokyo, Japan), which was maintained at 40℃. The mobile phase was acetonitrile : 0.1% phosphoric acid =8 : 52 (0–4 min), 35 : 65 (4–14 min) and 8 : 92 (14–20 min). The flow rate was adjusted to 1.0 mL/min. PABA, M-PABA, and E-PABA were detected at UV 280 nm.

2.8 Determination of bioavailability

Intravenous and oral administrations were performed in Wistar rats under anesthesia by intraperitoneal injection of three types of anesthesia (medetomidine, 0.375 mg/kg; butorphanol, 2.5 mg/kg; and midazolam, 2 mg/kg) to determine the bioavailability of PABA. In case of intravenous administration, PABA dissolved in physiological saline (PABA solution) was injected (5 μmol/kg) into the tail vein. Blood samples (0.2 mL) were collected from the jugular vein at predetermined intervals up to 3 h, and the same volume of saline was injected via the tail vein to prevent severe changes in the volume of distribution. For oral administration, PABA solution or LC-formulation (10 μmol/kg) was administered to rats, and blood (0.2 mL) was withdrawn from the jugular vein at intervals up to 6 h and the same volume of saline was injected via tail vein. Blood samples placed into heparinized tubes were immediately separated by centrifugation to obtain plasma (5 min, 4℃). Plasma and skin samples were stored at −30℃ until analysis.

2.9 *In vitro* skin permeation experiment

Full-thickness hairless rat skin was excised from the abdomen under anesthesia by *i.p.* injection of three types of anesthesia as above. Excess fat was trimmed off, and the skin samples were set in vertical-type diffusion cells with the epidermis side facing the donor compartment. PBS was applied to the receiver chamber as in the release experiment and maintained at 32℃. These skin permeation experiments were conducted after hydration for 60 min with PBS. Drug solution (1.0 mL) or its LC-formulation (1.0 mL) was applied to the donor cell to start the *in vitro* skin permeation experiment. An aliquot (500 μL) was withdrawn from the receiver chamber, and the same volume of PBS was added to the chamber to keep the volume constant. The skin permeation of Na-FL was determined using a fluorescence spectrophotometer.

2.10 Determination of *AUC*

The area under the plasma concentration–time curve (*AUC*) was calculated using the linear trapezoidal rule. The absolute bioavailability was determined as AUC_{po}/AUC_{iv} using the mean *AUC* values for oral and intravenous doses.

2.11 Statistical analysis

Statistical analysis was performed using unpaired Student's *t*-test (ANOVA), and p values less than 0.05 were considered to be significant.

3 Results

3.1 Homogeneity and visible appearance

First, the homogeneity and visible appearance of the prepared LC formulations were evaluated. Accepted formulations were a uniform opaque white mixture or uniform powder without visible signs of aggregates, whereas rejected formulations appeared as a non-uniform dispersion or aggregated wet powder. Figure 2 shows photographs to illustrate these criteria for accepted and rejected formulations. OP30, OM30, and OE30 were inconvenient for oral due administration because of the high percentage of lipid (creamy formulations); therefore, these formulations were not studied for oral administration. However, these formulations were accepted for topical application (TF30 and TF40). Non-uniform mixtures with aggregates were observed with a high percentage of LC-forming lipid (>40%); therefore, no further work was carried out with these formulations. Fine powders were obtained in OP10D, OM10D, and OE10D. However, when the MGE content increased to 20% (OP20D, OM20D, and OE20D, respectively), aggregated wet powders were observed. Therefore, no further work was carried out with them.

3.2 Particle size and zeta potential measurement

Table 3 shows particle size and zeta potential values of oral and topical LC formulations. The obtained results showed that the particle size tended to be smaller and the zeta potential became more negative with increasing MGE content. Formulations with low MGE content represented by 5% (i.e., OP5, OM5, OE5, and TF5) tended to have large particle size and low negative surface charge. Because the low surface charge indicated low stability of the 5% MGE

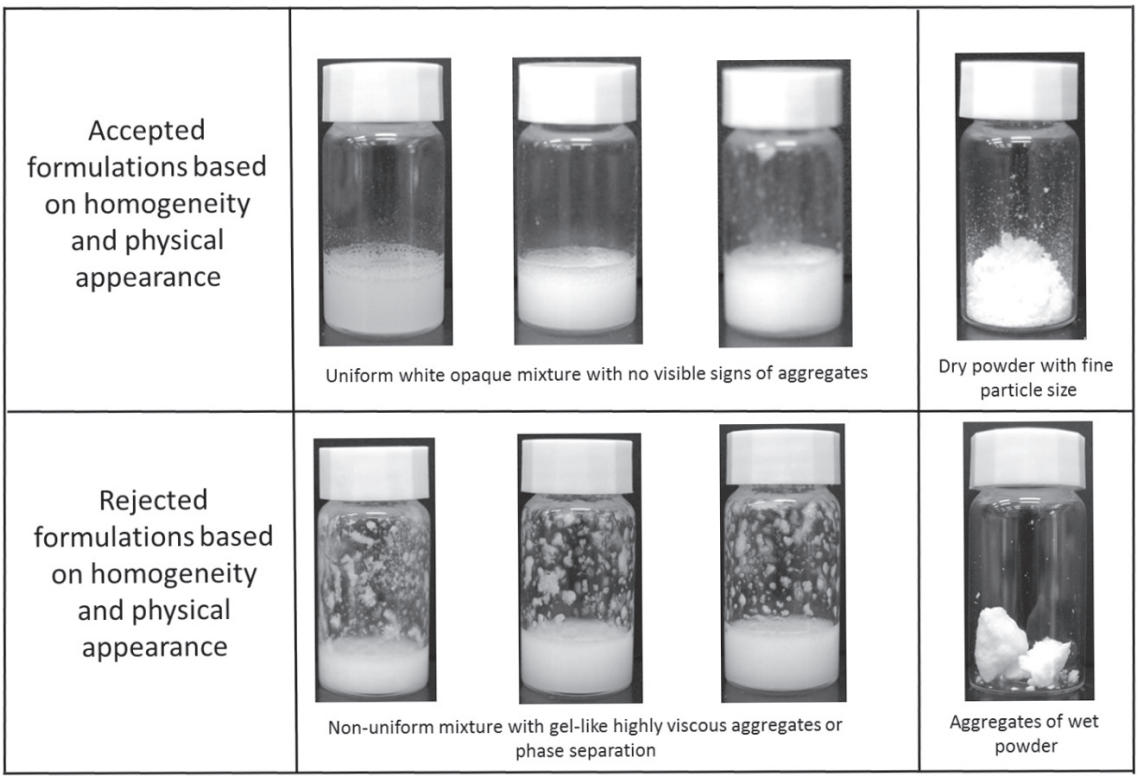

Fig. 2 Illustration photographs of accepted and rejected LC formulations based on homogeneity and visible appearance. Accepted formulations were appeared as a uniform opaque white mixture or uniform powder without visible signs of aggregates, while rejected formulations were appeared as a non-uniform dispersion or aggregated wet powder.

Table 3 Particle size (nm) and zeta potential (mV) of LC formulations.

Formulation code	Particle size (nm)	Zeta potential (mV)
OP5	409 ± 26	− 3.1 ± − 0.8
OP10	340 ± 21	− 10.4 ± − 1.7
OP20	288 ± 17	− 15.5 ± − 2.3
OP10D	366 ± 27	− 10.7 ± − 1.4
OM5	488 ± 23	− 2.8 ± − 0.7
OM10	327 ± 14	− 11.7 ± − 1.3
OM20	301 ± 29	− 16.2 ± − 2.4
OM10D	332 ± 27	− 6.9 ± − 1.1
OE5	412 ± 31	− 2.6 ± − 0.6
OE10	384 ± 28	− 12.4 ± − 1.8
OE20	311 ± 18	− 17.6 ± − 2
OE10D	377 ± 27	− 7.9 ± − 1.2
TF5	388 ± 22	− 3.1 ± − 0.7
TF10	348 ± 12	− 12.1 ± − 1.5
TF20	328 ± 26	− 17.4 ± − 1.3
TF30	351 ± 21	− 22.7 ± − 3.4
TF40	311 ± 17	− 30.4 ± − 4.2

Each value represents the mean ± S.E. of 3 experiments.

formulations, no further work was carried out with these formulations.

3.3 Drug release properties from LC formulations

Figure 3a-d shows the release profile of PABA, M-PABA, E-PABA, and Na-FL, respectively, from their LC formulations. All profiles obeyed Higuchi's law[15]: high correlation coefficients ($r>0.99$) were obtained for each formulation, indicating that *in vitro* drug release profiles of drug were fitted well with the square root Higuchi model.

For oral formulations, the amounts of PABA released from OP10D, OP10, OP20, and OP30 were 13.9 ± 2.5%, 23.7 ± 3.2%, 16.7 ± 2.8%, and 9.6 ± 0.8% (Fig. 3a), respectively, against the initial dosing. Those of M-PABA from OM10D, OM10, OM20, and OM30 were 6.4 ± 0.4%, 5.7 ± 0.3%, 4.2 ± 0.2%, and 3.4 ± 0.4% (Fig. 3b), respectively, and those of E-PABA from OM10D, OM10, OM20, and OM30 were 3.8 ± 0.3%, 3.4 ± 0.3%, 2.5 ± 0.2%, and 2.2 ± 0.2% (Fig. 3c), respectively. For topical formulations, the amounts of Na-FL released from TF10, TF20, TF30, and TF40 were 18 ± 0.6%, 15.5 ± 0.7%, 11.5 ± 0.6%, and 6 ± 0.7% (Fig. 3d), respectively.

Although the release profile was influenced by changes in the MGE concentration, it was influenced more dramatically by changes in the physiochemical properties of the entrapped drugs. For example, the release amount of Na-FL from TF10 was 18 ± 0.6% (Fig. 3d) as compared with the release of E-PABA from OE10, 3.8 ± 0.3% (Fig. 3c), although both formulations contained the same concentration of MGE.

3.4 SAXS chart of LC formulations

The phase structure of LC formulations was evaluated by SAXS. Figure 4a-c shows the X-ray diffraction profiles

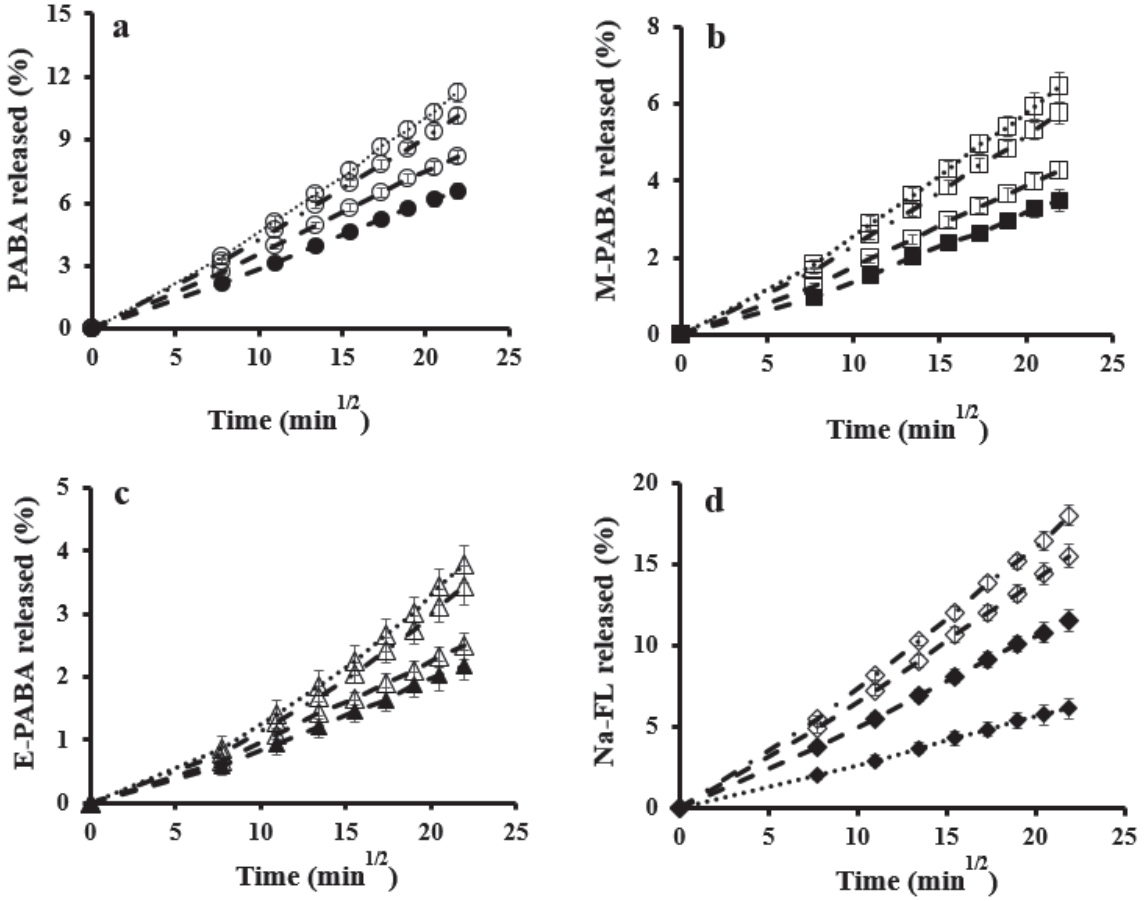

Fig. 3 Effect of LC forming lipid concentration and physiochemical properties of entrapped drug on the release profile of PABA (a), M-PABA (b), E-PABA (c) and Na-FL (d) from their LC formulations. Symbols: (a): (○+++), OP10D formulation; (○+−+), OP10 formulation; (○−−−), OP20 formulation; (●−−−), OP30 formulation; (b): (□+++), OM10D formulation; (□+−+), OM10 formulation; (□−−−), OM20 formulation; (■−−−), OM30 formulation; (c): (△+++), OE10D formulation; (△+−+), OE10 formulation; (△−−−), OE20 formulation; (▲−−−), OE30 formulation; (d): (◇+−+), TF10 formulation; (◇−−−), TF20 formulation; (◆−−−), TF30 formulation; (◆+++), TF40 formulation. Each point represents the mean ± S.E. of three experiments.

of OP10 (Fig. 4a), OP20 (Fig. 4b), and OM10 (Fig. 4c) formulations. Typical peaks reflection distance ratios at nearly 1, $\sqrt{3}$, and $\sqrt{4}$, revealed the presence of an H_2 inverted hexagonal phase. The same peaks reflection distance ratios were observed for OM20, OE10, OE20, TF10, TF20, TF30, and TF40 (data not shown). The phase behavior of these formulations was determined based on international tables for crystallography[16, 17]. Unidentified peaks were observed for oral dry powder LC formulations OP10D (Fig. 4d), OM10D (Fig. 4e) and OE10D (Fig. 4f).

3.5 Bioavailability of PABA

Figure 5 shows the time course of the plasma concentration of PABA after intravenous injection and Fig. 6 shows

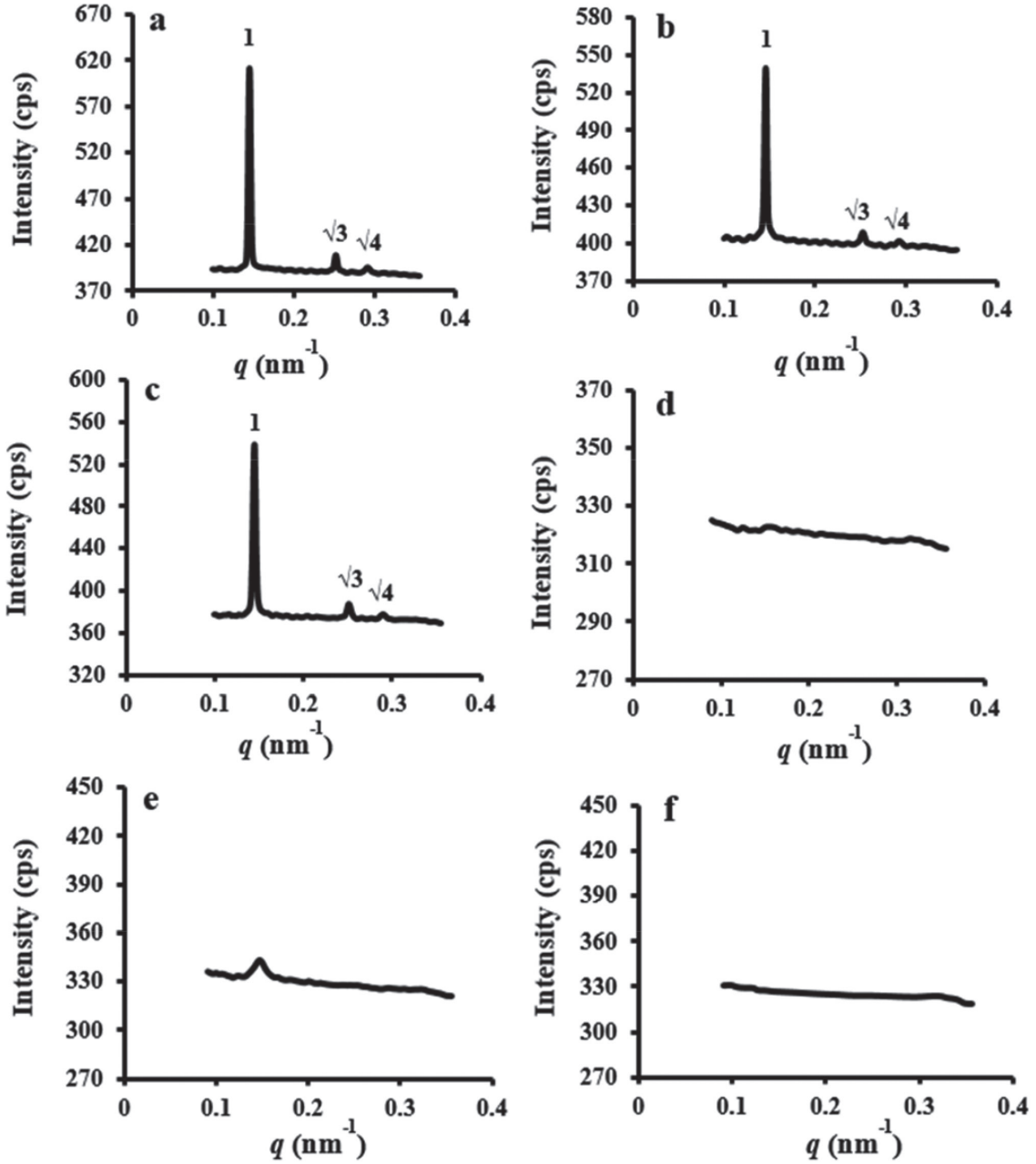

Fig. 4 SAXS charts of LC formulations: (a), OP10 formulation; (b), OP20 formulation; (c), OM10 formulation; (d), OP10D formulation; (e), OM10D formulation and (f), OE10D formulation. The peaks reflection distance ratios at: 1, $\sqrt{3}$, $\sqrt{4}$ confirming the presence of H_2 inverted hexagonal phase (a-c), the same peaks reflection distance ratios were observed for OM20, OE10, OE20, TF10, TF20, TF30 and TF40 (data were not shown). Unidentified peaks were observed for dry powder LC formulations (d-f).

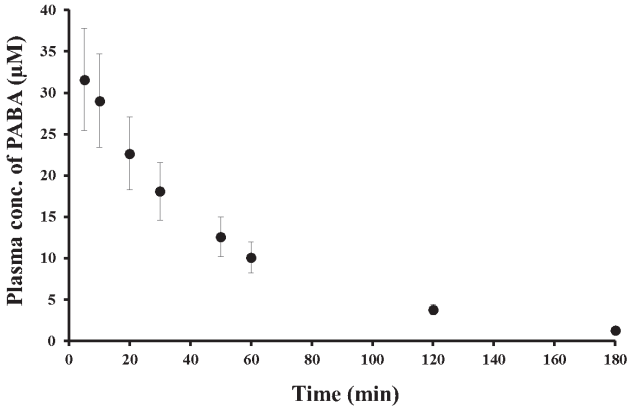

Fig. 5 Plasma profile after intravenous injection of PABA.

the time course of the plasma concentration of PABA after oral administration of its solution or PABA-, M-PABA-, and E-PABA-LC formulations in male Wistar rats. Table 4 summarizes the calculated $AUC_{0\text{-}6\ h}$, T_{max}, C_{max}, and absolute bioavailability (F) of PABA after oral administration.

The bioavailability after oral administration of OP20 (55 ± 13) (Fig. 6a), OM10 (44 ± 9) (Fig. 6b), and OE10 (43 ± 6) (Fig. 6c) was significantly higher than that of PABA solution (16 ± 2). No improvement was observed in the bioavailability for other LC formulations. The T_{max} of OP20 was faster compared with OM10 and OE10. The T_{max} of OE10 was delayed to 120 min. Only OP20, OM10, and OE10 showed significant improvement in the bioavailability of PABA. M-PABA, and E-PABA prodrugs after oral administration.

3.6 *In vitro* skin permeation profiles

Figure 7 shows the effect of LC formulations on the time course of the cumulative amount of Na-FL that permeated through hairless rat intact skin. Significant improvements in skin permeation of Na-FL was observed after application of TF20 and TF30 compared with that from the Na-FL solution. The enhancement ratios in the skin permeation for TF10, TF20, and TF30 formulations were 1.7, 4.3, and 2.9, respectively, but no improvement in skin permeation of the Na-FL was observed with TF40 formulation.

4 Discussion

Although LC formulations have received considerable attention because of their excellent potential as drug delivery systems[6], there seems to be a general lack of understanding among researchers regarding the effect of several factors such as physiochemical properties of the entrapped drugs, concentration of LC-forming lipids and LC phase structure on the oral and topical performance of these formulations. Therefore, the present study mainly focused on the developing strategies of oral and topical LC formula-

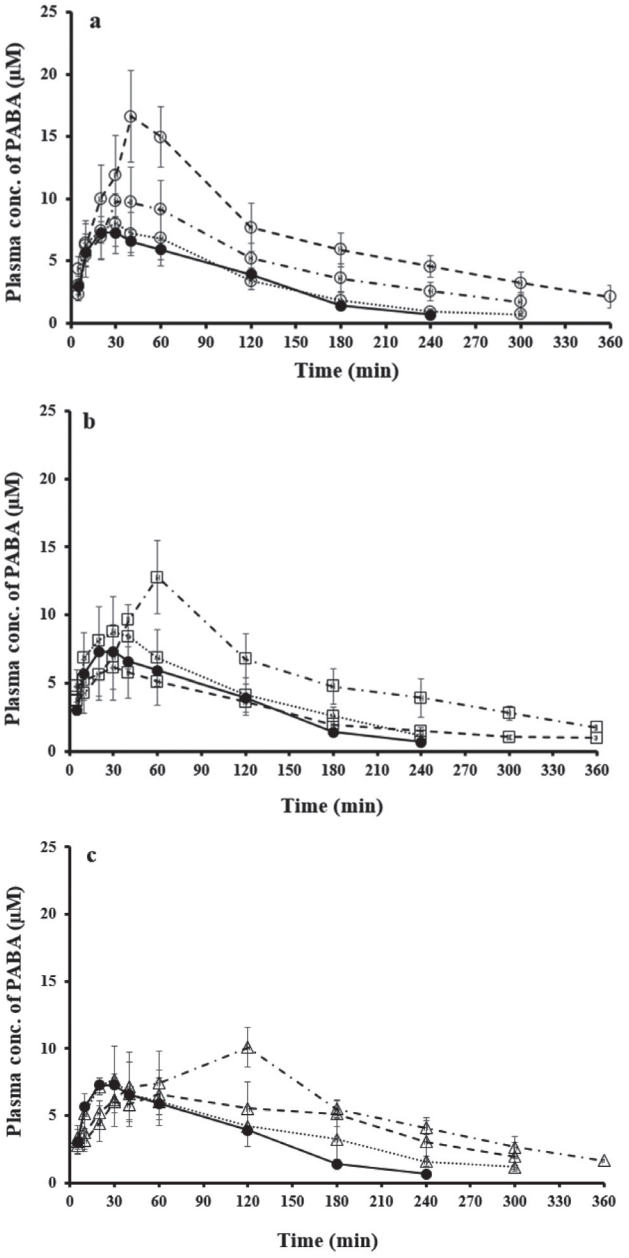

Fig. 6 Plasma profiles after oral administration of: (a), PABA-LC formulations; (b), M-PABA-LC formulations and (c), E-PABA-LC formulations. M-PABA and E-PABA were metabolized to PABA after oral administration. Symbols: (a): (○+++), OP10D formulation; (○+−+), OP10 formulation; (○−−−), OP20 formulation; (●−), PABA solution; (b): (□+++), OM10D formulation; (□+−+), OM10 formulation; (□−−−), OM20 formulation; (c): (△+++), OE10D formulation; (△+−+), OE10 formulation; (△−−−), OE20 formulation. Each point represents the mean ± S.E. of three experiments.

Table 4 Bioavailability of PABA after oral administration.

	$AUC_{0\text{-}6\ h}$	T_{max} (min)	C_{max} (μM)	MRT (min)	$F_{0\text{-}6\ h}$ (%)
PABA solution	876 ± 109	27 ± 6	7.4 ± 0.9	11 ± 1.8	16 ± 2
OP10	1595 ± 440	37 ± 6	10 ± 2.7	12.7 ± 2	30 ± 8
OP20	2939 ± 700*	46 ± 11	16 ± 3	15 ± 2.5	55 ± 13*
OP10D	1047 ± 260	33 ± 6	8 ± 2	11.4 ± 1	19 ± 4
OM10	2366 ± 496*	53 ± 11	12 ± 2.5	14 ± 2.1	44 ± 9*
OM20	1167 ± 261	33 ± 6	6 ± 2	11.8 ± 2	21 ± 5
OM10D	1072 ± 295	33 ± 6	8.8 ± 2.6	11.5 ± 2	20 ± 5
OE10	2314 ± 348*	120 ± 21	10 ± 1.5	13 ± 2.5	43 ± 6*
OE20	1519 ± 516	53 ± 11	6.5 ± 1.8	12.3 ± 3	28 ± 9
OE10D	1208 ± 348	23 ± 6	7.8 ± 2	12.1 ± 1	26 ± 6

Each value shows the mean ± S.E. of 3 experiments.
AUC: Area under the plasma concentration-time curve.
T_{max}: Time to reach maximum plasma concentration.
C_{max}: Maximum plasma concentration.
MRT: Mean residence time.
F: Absolute bioavailability (AUC_{po}/AUC_{iv}).
*: Significantly different from PABA solution $p < 0.05$ (Student's *t*-test).

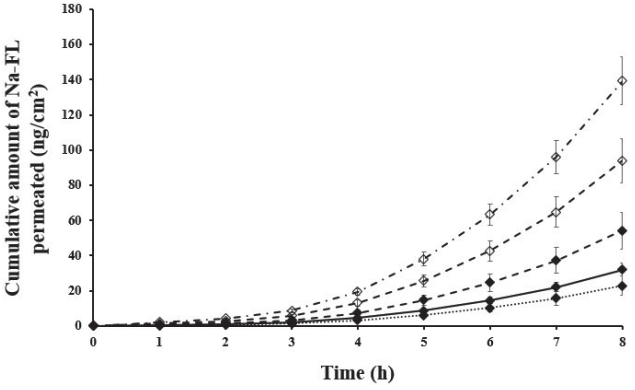

Fig. 7 Effect of LC forming lipid concentration on the time course of the cumulative amount of Na-FL. Symbols: (◆---), TF10 formulation; (◇+-+), TF20 formulation; (◇---), TF30 formulation; (◆+++), TF40 formulation; (◆−), Na-FL solution. Each point represents the mean ± S.E. of three experiments.

tions by investigating the effect of such factors to improve the performance of these formulations.

MGE was selected an LC forming lipid because of its low viscosity, stability and better drug absorption enhancer compare with other LC forming lipids[13]. We initially screened various oral and topical LC formulations (Table 2). The obtained results on their homogeneity and visible appearance (Fig. 2) showed that it was not recommended to prepare oral LC dispersions with MGE at a concentration of more than 30%, because these formulations tended to be too viscous and inconvenient for oral administration. When the concentration of MGE was above 40%, LC was aggregated with phase separation, therefore, they were inconvenient for both oral and topical formulations. In addition, MGE was not recommended to prepare LC dry powder at a concentration of 20% or above.

Zeta potential is an important parameter for the evaluation of stability and bio-distribution[18, 19]. By increasing the MGE concentration, the particle size tended to be smaller and the zeta potential became more negative (Table 3), suggesting that the number of LC forming particles was increased with an increasing of MGE concentration. The negative zeta potential of LC formulations was due to the present of free oleic acid in the lipid phase. The negative charge can also be explained by preferential adsorption of hydroxyl ions at the lipid-water interface.

As demonstrated in Fig. 3, the drug release profiles from LC formulations were influenced by the concentration of MGE and the physiochemical properties of the entrapped drugs. These results indicated that the drug diffusivity in the formulation decreased with an increase in MGE concentration. The drug diffusivity was affected more dramatically by changes in the physiochemical properties of entrapped drugs. The released amount of Na-FL from TF10 was 18 ± 0.6% compared with the release of E-PABA from OE10 (3.8 ± 0.3%), although both formulations contained the same concentration of MGE (Fig. 3a-d). A similar phenomenon was observed with other drugs (PABA and M-PABA), and drug release decreased with an increase in lipophilicity. Figure 8 schematically explains the effect of

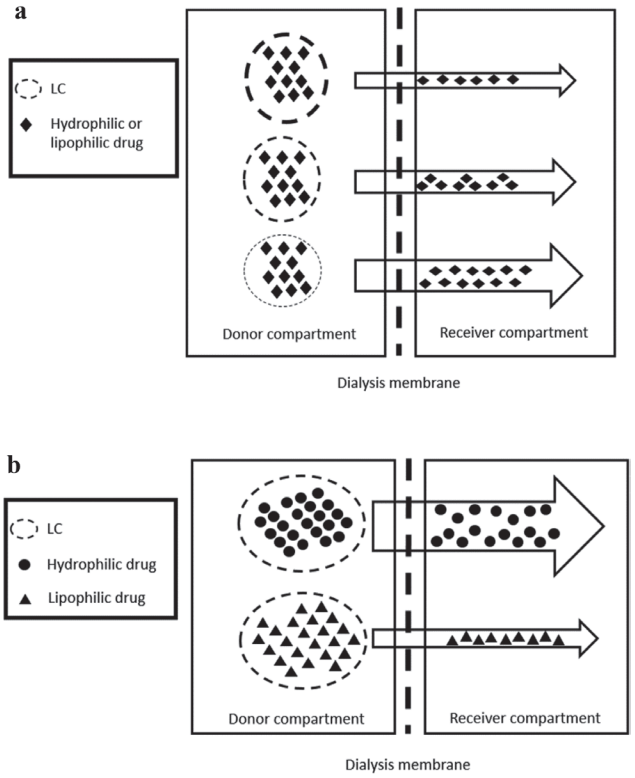

Fig. 8 Illustrations explaining the effect of LC concentration (a) and the physiochemical properties of entrapped drug (b) on the drug release amount. The release amount of drug is increased by a decrease of LC concentration (a). The release amount of drug is more dramatically increased by a decrease of the drug lipophilicity (b).

lipid concentration and the physiochemical properties of entrapped drugs on drug release.

Typical reflection patterns at nearly 1, $\sqrt{3}$, and $\sqrt{4}$ for oral dispersions and topical LC formulations indicated that these formulations successfully managed to form an H_2 inverted hexagonal phase (Fig. 4a-e). Previous studies[20, 21] have reported that the hexagonal phase has several advantages. It has a larger surface area to interact with biological membranes with high fluidity, and greater amounts of drugs can be incorporated independent of their solubility. In contrast to our findings, other studies have demonstrated the presence of cubosomes using different types of LC-forming lipids such as glyceryl monooleate (GMO) or phytantriol (PHT)[10, 22]. We strongly believed that several factors might affect the phase structure of LC formulations, such as temperature, type of LC-forming lipid, physiochemical properties of the entrapped drugs, lipid concentration, and type of surfactant. Further studies are necessary to understand in full the effect of such factors on the phase transition of LC formulations. The key point is to successfully prepare hexosomes or cubosomes by design with LC formulations. No clear mechanism or clear evidence has been proposed to indicate that cubosomes have more potential than hexosomes, or vice versa, as a drug delivery system. On the other hand, unidentified peaks were observed in the SAXS measurement of oral dry powder formulations (Fig. 4e-f).

The drug absorption from oral LC formulations was dramatically affected by the MGE concentration and the physiochemical properties of entrapped drugs (Fig. 6). The bioavailability of PABA was significantly improved by the 20% MGE formulation (OP20) compared with other LC formulations or PABA solution alone (Fig. 6a). These results indicated that the rate limiting step in the absorption of hydrophilic drugs must be the permeating process through the intestinal membrane. Thus, the hexosome particles in contact with the small intestine were high in this formulation (OP20) by increasing the MGE concentration.

In contrast, in case of M-PABA and E-PABA entrapping formulations, a low concentration of MGE (OM10 and OE10) significantly improved the bioavailability of PABA compared with other LC formulations or PABA solution alone (Fig. 6b and c). These results indicated that the rate limiting step in the absorption process for lipophilic drugs with LC formulations must be their release rate. Thus, the release amount of these drugs increased from these formulation (OM10 and OE10) by decreasing the MGE concentration. This could be also the reason why the absorption of M-PABA and E-PABA from the LC formulations were delayed compared with PABA-LC formulation (Table 4). Furthermore, M-PABA and E-PABA were metabolized to PABA after oral administration of their LC formulations, indicating that LC systems were unable to protect these drugs from intestinal esterase metabolite activity.

Dry powdered oral LC formulations did not manage to form hexosomes or cubosomes, which could be a reason why these formulations were unable to improve the bioavailability of PABA.

In consequence, the same as in the *in vivo* oral absorption, *in vitro* skin permeation results were dramatically affected by the MGE concentration. Significant improvement in the skin penetration of Na-FL was observed in 20% and 30% MGE (TF20 and TF30) with enhancement ratios of 4.3 and 2.9, respectively. However, no marked improvement was observed in 10% and 40% MGE, suggesting that a low concentration of MGE such as 10% (TF10) could lead to a reduction in hexosomes particles. Thus it is necessary to overcome the barrier function of stratum corneum. On the other hand, a high concentration of MGE such as 40% (TF40) reduced drug release from the formulation (Fig. 7).

The detailed mechanism of the enhanced oral drug absorption and transdermal drug penetration by LC systems is not fully understood yet[9, 23]. Further studies must be conducted to clarify the absorption-enhancing mechanism

of LC formulations.

5 Conclusion

The present data showed that LC formulations are promising to improve oral absorption and transdermal penetration of drugs. Our findings showed that the concentrations of LC-forming lipid and the physiochemical properties of entrapped drugs are very important factors that should be considered by researchers in this field to improve the performance of LC formulations in various pharmaceutical applications. Understanding the effect of these factors on LC formulation performance could enable researchers to develop LC formulation approaches that intended to improve the oral absorption and skin permeation of drugs.

References

1) Ericsson, B.; Eriksson, P.O.; Lofroth, J.E.; Engstrom, S. Cubic phases as delivery systems for peptide drugs. *ACS Symp. Ser.* **469**, 252-263(1991).
2) Kadhum, W.R.; Todo, H.; Sugibayashi, K. Skin permeation: Enhancing ability of liquid crystal formulations. in *Percutaneous penetration enhancers chemical methods in penetration enhancement: Drug Manipulation Strategies and Vehicle Effects*(Dragicevic-Curic, N.; Maibach, H. eds.). Springer-Verlag, Berlin, Heidelberg, pp. 243-253(2015).
3) Wallin, R.; Engstrom, S.; Mandenius, C.F. Stabilisation of glucose oxidase by entrapment in a cubic liquid crystalline phase. *Biocatalysis* **8**, 73-80(1993).
4) Nylander, T.; Mattisson, C.; Razumas, V.; Miezes, Y.; Hakansson, B. A study of entrapped enzyme stability and substrate diffusion in a monoglyceride-based cubic liquid crystalline phase. *Colloids Surf. A* **114**, 311-320(1996).
5) Caboi, F.; Nylander, T.; Razumas, V.; Talaikyte, Z.; Monduzzi, M.; Larsson, K. Structural effects, mobility, and redox behavior of vitamin K1 hosted in the monoolein:water liquid crystalline phases. *Langmuir* **13**, 5476-5483(1997).
6) Guo, C.; Wang, J.; Cao, F., Lee, R.J.; Zhai, G. Lyotropic liquid crystal systems in drug delivery. *Drug Discov. Today* **15**, 1032-1040(2010).
7) Dae, G.L.; Won, W.J.; Nam, A.K.; Jun, Y.L.; Seol, H.L.; Woo, S.S.; Nae, G.K.; Seong, H.J. Effect of the glyceryl monooleate-based lyotropic phases on skin permeation using in vitro diffusion and skin imaging. *Asian J. Pharm. Sci.* **9**, 324-329(2014).
8) Lopes, L.B.; Speretta, F.F.; Bentley, M. Enhancement of skin penetration of vitamin K using monoolein-based liquid crystalline systems. *Eur. J. Pharm. Sci.* **32**, 209-215(2007).
9) Okawara, M.; Hashimoto, F.; Todo, H.; Sugibayashi, K.; Tokudome, Y. Effect of liquid crystals with cyclodextrin on the bioavailability of a poorly water-soluble compound, diosgenin, after its oral administration to rats. I*nt. J. Pharm.* **472**, 257-261(2014).
10) Nguyen, T.H.; Hanley, T.; Porter, C.J.; Boyd, B.J. Nanostructured liquid crystalline particles provide long duration sustained-release effect for a poorly water soluble drug after oral administration. *J. Control. Release* **153**, 180-186(2011).
11) Ali, A.; Kataoka, N.; Ranneh, A.; Iwao, Y.; Noguchi, S.; Oka, T.; Itai, S. Enhancing the solubility and oral bioavailability of poorly water-soluble drugs using monoolein cubosomes. *Chem. Pharm. Bull.* **65**, 42-48 (2017).
12) Cohen-Avrahami, M.; Aserin, A.; Garti, N. HII mesophase and peptide cell-penetrating enhancers for improved transdermal delivery of sodium diclofenac. *Colloids Surf. B Biointerfaces* **77**, 131-138(2010).
13) Kadhum, W.R.; Oshizaka, T.; Hijikuro, I.; Todo, H.; Sugibayashi, K. Usefulness of liquid–crystal oral formulations to enhance the bioavailability and skin tissue targeting of p-amino benzoic acid as a model compound. *Eur. J. Pharm. Sci.* **88**, 282-290(2016).
14) Yamada, K.; Yamashita, J.; Todo, H.; Miyamoto, K.; Hashimoto, S.; Tokudome, Y.; Hashimoto, F.; Sugibayashi, K. Preparation and evaluation of liquid crystal formulation having skin permeation-enhancing ability of the entrapped drug. *J. Oleo Sci.* **60**, 31-40 (2011).
15) Higuchi, T. Mechanism of sustained action medication: theoretical analysis of rate of release of solid drugs dispersed in solid matrices. *J. Pharm. Sci.* **52**, 1145-1148(1963).
16) Anderson, D.M.; Gruner, S.M.; Leibler, S. Geometrical aspects of the frustration in the cubic phases of lyotropic liquid crystals. *Proc. Natl. Acad. Sci. USA* **85**, 5364-5368(1988).
17) Qiu, H.; Caffrey, M. The phase diagram of monoolein/water system: metastability and equilibrium aspects. *Biomaterials* **21**, 223-234(2000).
18) Sherif, S.; Bendas, E.R.; Badawy, S. The clinical efficacy of cosmeceutical application of liquid crystalline nanostructured dispersions of alpha lipoic acid as anti-wrinkle. *Eur. J. Pharm. Biopharm.* **86**, 251-259 (2014).
19) Weiss, V.M.; Naolou, T.; Hause, G.; Kuntsche, J.; Kressler, J.; Mader, I. Poly(glycerol adipate)-fatty acid esters as versatile nanocarriers: from nanocubes over ellipsoids to nanospheres, *J. Control. Release* **158**, 156-164(2012).
20) Siekmann, B.; Bunjes, H.; Koch, M.H.J.; Westesen, K. Preparation and structural investigations of colloidal

dispersions prepared from cubic monoglycerideYwater phases. *Int. J. Pharm.* **244**, 33-43(2002).
21) Esposito, E.; Eblovi, N.; Rasi, S.; Drechsler, M.; Di Gregorio, G.; Menegatti, E.; Cortesi, R. Lipid-based supramolecular systems for topical application: a preformulatory study. *AAPS PharmSciTech.* **5**, 1-15(2003).
22) Hinton, T.M.; Grusche, F.; Acharya, D.; Shukla, R.; Bansal, V.; Waddington, L.J.; Monaghan, P.; Muir, B.W. Bicontinuous cubic phase nanoparticle lipid chemistry affects toxicity in cultured cells. *J. Toxicol. Res.* **3**, 11-22(2014).
23) Uchino, T.; Murata, A.; Miyazaki, Y.; Oka, T.; Kagawa, Y. Glyceryl monooleyl ether-based liquid crystalline nanoparticles as a transdermal delivery system of flurbiprofen: characterization and in vitro transport. *Chem. Pharm. Bull.* **63**, 334-340(2015).